

Novel fidaxomicin antibiotics through site-selective catalysis

David Dailler^{1,4}, Andrea Dorst^{1,4}, Daniel Schäfle², Peter Sander^{2,3} & Karl Gademann¹  ¹✉

Fidaxomicin (FDX) is a marketed antibiotic for the treatment of *Clostridioides difficile* infections (CDI). Fidaxomicin displays antibacterial properties against many Gram-positive bacteria, yet the application of this antibiotic is currently limited to treatment of CDI. Semisynthetic modifications present a promising strategy to improve its pharmacokinetic properties and also circumvent resistance development by broadening the structural diversity of the derivatives. Here, based on a rational design using cryo-EM structural analysis, we implement two strategic site-selective catalytic reactions with a special emphasis to study the role of the carbohydrate units. Site-selective introduction of various ester moieties on the noviose as well as a Tsuji–Trost type rhamnose cleavage allow the synthesis of novel fidaxomicin analogs with promising antibacterial activities against *C. difficile* and *Mycobacterium tuberculosis*.

¹Department of Chemistry, University of Zurich, Zurich, Switzerland. ²Institute of Medical Microbiology, University of Zurich, Zurich, Switzerland. ³National Center for Mycobacteria, University of Zurich, Zurich, Switzerland. ⁴These authors contributed equally: David Dailler, Andrea Dorst. ✉email: karl.gademann@chem.uzh.ch

Fidaxomicin (**1**, tiacumicin B, lipiarmycin A3) constitutes an 18-membered narrow-spectrum macrolide antibiotic that was extracted from several actinomycetes^{1–7} and shows antibacterial properties against mainly Gram-positive bacteria⁸, in particular against methicillin-resistant *Staphylococcus aureus*⁹, multidrug-resistant *Mycobacterium tuberculosis*⁷, and *Clostridioides difficile*^{10–12}. To date, the clinical use is limited to the treatment of *C. difficile* infections, the main cause of hospital-acquired diarrhea, against which fidaxomicin was approved by the FDA in 2011^{13–17}. Fidaxomicin inhibits the RNA polymerase (RNAP) via a new mechanism of action, rendering second-generation derivatives thereof particularly attractive^{18–20}. Resistance development in bacteria accelerated over the last few decades and new mechanisms of resistance have emerged, which calls for the development of antibiotics with unique mechanisms of action²¹.

Globally, an estimated 10.0 million people fell ill with tuberculosis (TB) in 2019 and more than 1 million people died of it. Drug-resistant TB continues to be a public health threat. Almost half a million people developed rifampicin-resistant TB (RR-TB), of which 78% were multidrug resistant (MDR)²². Multidrug-resistant *M. tuberculosis* strains exhibit resistance toward the two most effective drugs, isoniazid and rifampicin, of the four drug standard treatment regimen. Alarmingly, in some countries, more than 50% of previously treated TB cases had MDR/RR-TB. Patients suffering from MDR-TB require a treatment with second-line drugs, which are less effective, more toxic, and more expensive. New treatment regimens combining compounds with novel mode of actions like bedaquiline²³ and repurposed drugs (linezolid) are currently evaluated for the treatment of MDR-TB²⁴. However, resistant strains were detected soon after approval of novel drugs²⁵. These findings indicate that the TB drug-pipeline has to be fueled continuously.

Susceptibility of *C. difficile* to fidaxomicin remains generally very high in the clinic, although there have been very few cases of fidaxomicin-resistant strains emerging^{26,27}, which calls for the development of second-generation derivatives. Although fidaxomicin has a high potential to deliver next-generation antibiotics, there are only few successful approaches toward new derivatives documented that might broaden structure–activity relationship (SAR) information and thereby further extend its application^{18,28,29}. So far, most known derivatives were obtained through fermentation of gene-knockout mutants of the producer strain or by chemical modification of the homoorsellinic acid moiety^{30–35}. Furthermore, several compounds with a similar scaffold were found along with fidaxomicin (**1**), some of which lack the rhamnose-orsellinate and/or the noviose moiety^{8,36}. Those truncated products missing one of the sugar moieties display significantly decreased antibiotic activity and thereby point out the importance of these carbohydrate units³⁷. Interestingly, nature also provides similar scaffolds from other species, such as mangrolide A (**2**) and D (**3**) that possess different sugar moieties and a similar macrolactone (Fig. 1)^{38,39}. Total syntheses campaigns of these compounds were started and successfully accomplished, but not answering the intriguing question on the role of the carbohydrate units^{40–44}.

Over the past few decades, derivatization of natural products has been demonstrated to be an effective approach for the development of new drug candidates²¹. However, the direct and selective functionalization of these scaffolds to gain specific SAR information still remains challenging due to their structural complexity and broad variety of functional groups. In order to address these issues, chemo- and site-selective functionalization recently emerged as a particularly appealing approach⁴⁵. Especially, site-selective transition-metal catalysis and organocatalysis started to find widespread application in derivatization of natural products⁴⁶. In this study, we report on the generation of novel fidaxomicin derivatives through site-selective catalysis using a rational design based on a cryo-electron microscopy (cryo-EM) structure of fidaxomicin binding to *M. tuberculosis* RNAP^{18,19}. In this context, semisynthetic strategies for the modification of fidaxomicin on the noviose- as well as on the rhamnose-orsellinate moiety were developed: (1) the application of site-selective organocatalysis for the generation of a library of 3''-acylated fidaxomicin derivatives and (2) a palladium-catalyzed allylic substitution for the selective cleavage of the rhamnose-resorcyate moiety. By these strategies, potent fidaxomicin derivatives that cannot be obtained by genetic modification could be prepared by chemical synthesis.

Results and discussion

Design based on cryo-EM structural analysis. Previous studies on the fermentation conditions led to the isolation of several fidaxomicin congeners with different ester moieties in various positions on the noviose moiety⁴⁷. These analogs displayed decreased antibiotic activities compared to the isobutyric ester moiety in 4''-position of the parent compound. Intriguingly, isobutyric ester migration to 3''-position (tiacumicin F) did not lead to a significant decrease of activity^{3,5,8}, which is in agreement with the recently disclosed cryo-EM structure. Indeed, there is an “open space” toward the C3''-hydroxy group that allows the introduction of functional groups (Fig. 2a, b). In contrast, the C4''-isobutyric ester fits perfectly into this pocket, but the space for further modifications in this position is limited. Moreover, potential interaction with or replacement of water in the active site constitutes a promising strategy that has already been demonstrated to be beneficial in drug design^{48–50}. Finally, the C2''-hydroxy group is involved in multiple hydrogen-bonding interactions between Arg412 and acetal of the noviose moiety (Fig. 2c)^{18,19}. Therefore, we expect C2''-acylation of fidaxomicin derivatives to have a detrimental effect on their bioactivity. Thus, we hypothesized that modifications on the C3''-hydroxy group of fidaxomicin constitute a viable design strategy that could lead to retained or enhanced bioactivity.

On the other part of fidaxomicin, several hydrogen-bonding interactions of Arg89 with the rhamnose moiety and Lys1101 with the phenolic hydroxy group on the homoorsellinic acid moiety as well as a cation- π interaction of Arg84 with the aromatic moiety are present (Fig. 3). Therefore, we aimed to study the influence of variations on the rhamnose-resorcyate moiety by modifying this part of the lead structure.

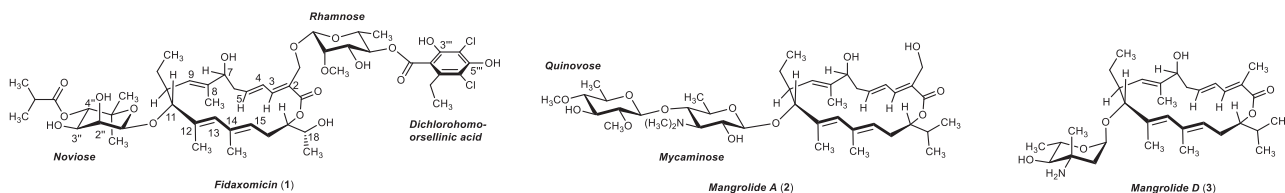


Fig. 1 Glycosylated macrocyclic antibiotics. Structures of fidaxomicin (**1**), mangrolide A (**2**), and D (**3**).

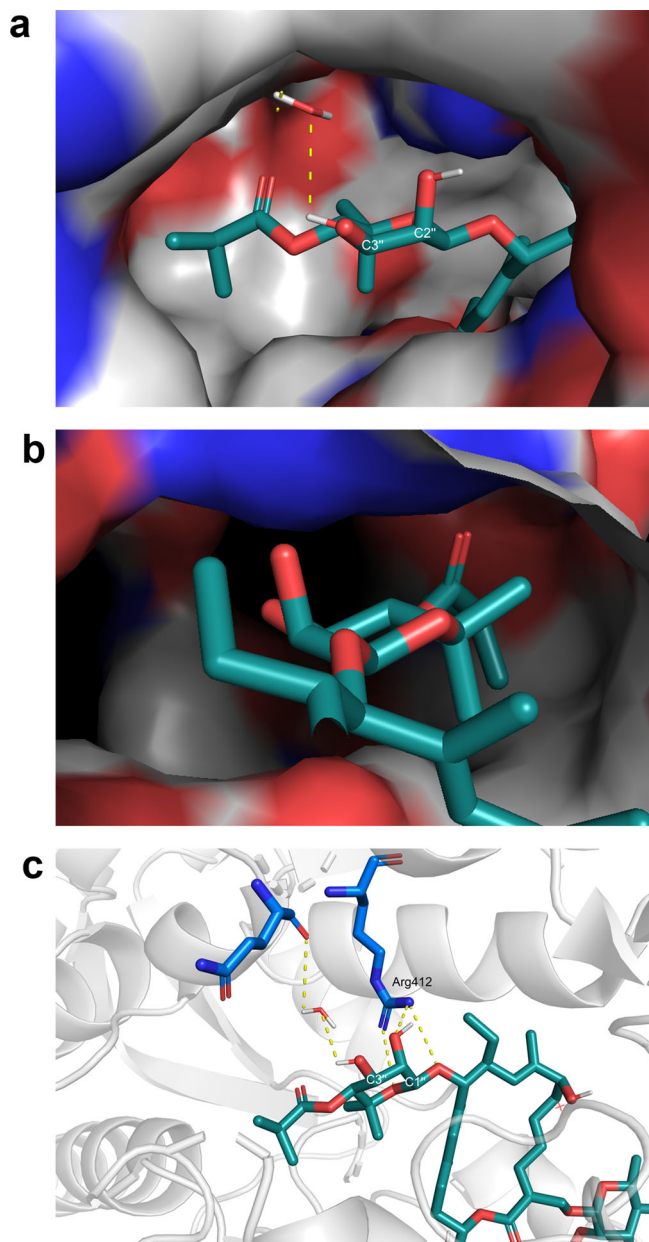


Fig. 2 Cryo-EM structure of fidaxomicin binding to *M. tuberculosis* RNAP (PDB ID: 6FBV)¹⁸. **a** Fidaxomicin (cyan), protein (surface representation/gray). Interaction of C3'-OH with H₂O. Limited space around isobutyric ester moiety. **b** Detailed view on the binding pocket of fidaxomicin's noviose moiety. C3'-OH points toward an "open space." C4'-isobutyric ester fits into its pocket. **c** Detailed view on the interactions of the noviose part to the protein. C2'-OH is blocked by an interaction with Arg412 (blue).

Modifications on the noviose unit. As discussed above, careful analysis of the cryo-EM structure of fidaxomicin binding to *M. tuberculosis* RNAP and previously reported bioactivities prompted us to consider selective C3'-acylation of the noviose moiety to gain SAR and potentially identify novel lead structures for drug discovery. Given the nature and high number of hydroxy groups in OP1118 (**4**), a degradation metabolite of fidaxomicin (**1**), as well as the lack of data concerning their reactivities and the chemical fragility of fidaxomicin, site-selective functionalization of C3'-OH represents an interesting challenge (Fig. 4)⁵¹.

In order to address this reactivity challenge, we envisioned to apply non-enzymatic methodology⁵². Over the past 15 years,

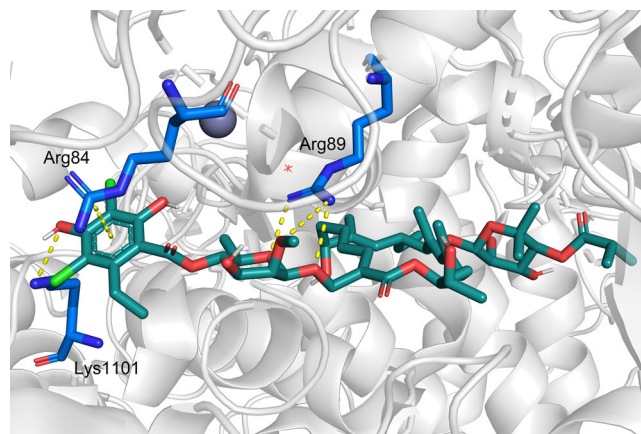


Fig. 3 Cryo-EM structure of fidaxomicin binding to *M. tuberculosis* RNAP (PDB ID: 6FBV)¹⁸. Fidaxomicin (cyan), protein (gray), and amino acid residues (blue). Detailed view on the interactions of the rhamnose-resorcyate part to the protein.

extensive research efforts led to the development of efficient and complementary synthetic methods to access regioselective functionalization of carbohydrate hydroxy groups⁵³. Analysis of the structural feature of fidaxomicin allowed us to identify the *cis*-vicinal diol as a potential platform for catalysis based on reversible covalent interactions of organoboron compounds. Indeed, this approach enabled by molecular recognition has proven to be effective for various transformations^{54,55}. In addition to provide high regioselectivity, this strategy would also potentially outcompete the initially more reactive secondary hydroxy groups (C7-OH/C18-OH) through activation of the *cis*-vicinal diol via tetracoordinate borate, therefore avoiding undesired over-acylation⁵⁶. In order to study the feasibility of this transformation, we thus started with the synthesis of the required precursor for catalysis. Considering the inherently higher nucleophilicity of phenol moiety, we thus turned our attention to the synthesis of bisallyl-OP1118 (**5**) (Fig. 5). Starting from commercially available fidaxomicin (**1**), cleavage of the isobutyrate ester via methanolysis followed by bisallyl protection of the phenol moiety afforded the starting compound for catalysis in 71% over two steps.

With the required starting material in hand, we turned our attention to the screening of initially described ethanolamine ester of diphenylborinic acid catalyst (Taylor's catalyst)⁵⁶ along with a boronic acid catalyst recently developed by Shimada et al.⁵⁷. Under classic conditions, both catalysts afforded conversion to the desired product (Fig. 6).

Encouraged by this finding, we therefore optimized the reaction with the Shimada catalyst since it offered slightly higher catalytic activity in these initial experiments. After screening of all the parameters of the reaction, we were able to obtain full conversion (UHPLC/MS analysis) to the desired compound **7** (confirmed by 2D NMR analysis; see Supplementary Fig. 10, section NMR Spectra) with the conditions depicted in Fig. 7.

Noteworthy, control experiments without catalyst confirming its presence are essential to ensure high conversion and site-selectivity. Moreover, the temperature (50 °C) is elevated compared to previously reported conditions; this is crucial to achieve complete conversion, which might arise from steric hindrance or conformational aspects imputed to the *gem*-dimethyl moiety of the noviose. Finally, subsequent deprotection of the allyl moiety in a one-pot two-step manner allowed us to obtain the desired product **7** in 67% yield (for experimental details refer to the Supplementary Methods). As expected,

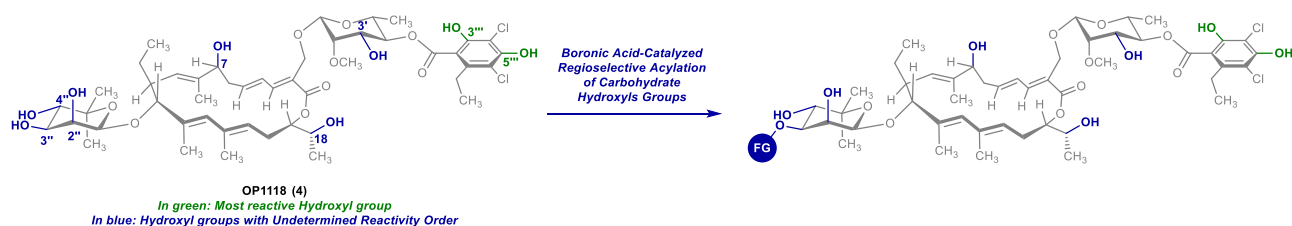


Fig. 4 Site-selective acylation of **4**. Overview of the strategy.

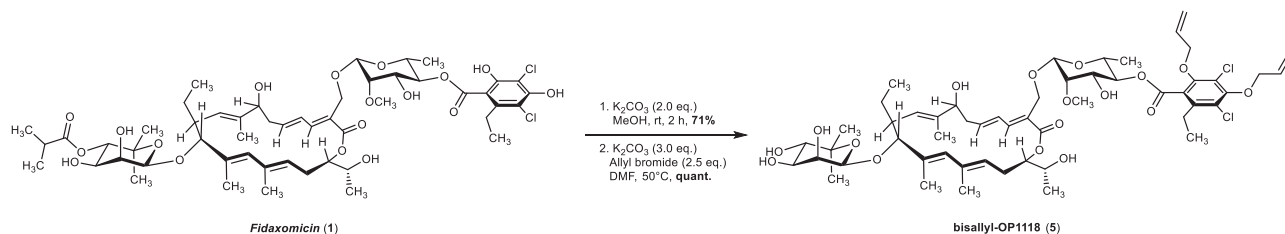


Fig. 5 Preparation of the catalysis-precursor bisallyl-OP1118 (**5**). Synthesis of **5** from natural product **1** via isobutyl ester hydrolysis and allyl protection.

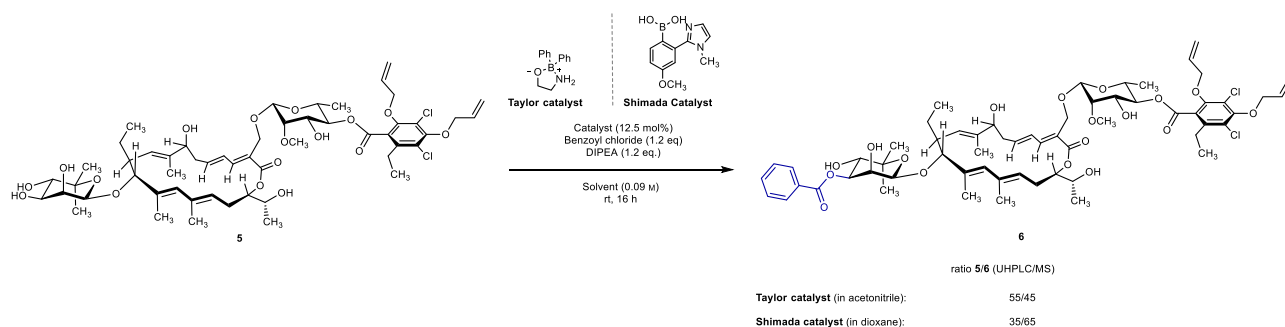


Fig. 6 C3''-OH acylation of **5**. Initial catalyst evaluation to access C3''-acylated fidaxomicin derivatives.

attempts to perform this selective C3''-acylation directly with the compound OP1118 (**4**) led to the functionalization of the dichlorohomo-orsellinic acid moiety. Furthermore, experiments with bisallyl-fidaxomicin⁵¹ were performed in order to study C4''-C3''-diacylated fidaxomicin derivatives. Unfortunately, we were not able to observe any traces of the desired functionalization even with stoichiometric amount of the organocatalyst. This could be explained by the steric hindrance caused by the C4''-isobutyrate moiety close to the reactive site. With the optimized conditions in hand, we turned our attention to the delivery of a library of C3''-acylated fidaxomicin derivatives. First, benzoyl chloride derivatives with different substitution patterns were screened. We were pleased to find that *ortho*-, *meta*-, and *para*-substitutions are tolerated, in addition to electron withdrawing and electron donating groups **7a–f**. Moreover, in some cases (**7d–f**), concomitant formation of C2''-benzoylated fidaxomicin derivatives (confirmed by 2D NMR analysis; see Supplementary Fig. 28) were observed in not negligible amount. Presumably, the C2''-benzoylated compounds arise from competing activation of the second hydroxy group of the *cis*-vicinal diol rather than benzoyl migration, as resubmission of the C3''-acylated fidaxomicin to the reaction conditions did not lead to any isomerization. Gratifyingly, the C2''/C3''-benzoylated fidaxomicin mixture was separable by preparative HPLC purification, allowing us to gain more SAR information. Heteroaromatic scaffolds were also introduced successfully with almost exclusive regioselectivity to afford compounds **7j–n** in medium to high yield, except the pyridine moiety **7i**. Preliminary interesting biological activities for the 3-furoyl derivatives **7j** led us to explore the impact of the substitution of the latter, leading to structures **7o–r**. In

consideration of the bioactivities of tiacumicin F (**7u**), we envisioned to study non-aromatic C3''-acylated fidaxomicin derivatives. While C3''-acylated fidaxomicin derivatives **7s–t** were obtained in good yield at 10 °C to control overreaction and degradation (THF ring formation)⁵¹, increase of substitution at carbon α to the carbonyl led to degradation of the reactivity. This highlighted the crowded environment of the noviose, which is in line with previous observations made during the optimization of the reaction conditions. To ensure generation of sufficient amounts for subsequent biological evaluation, we therefore increased the amount of Shimada catalyst in the most difficult cases to afford tiacumicin F (**7u**) and compounds **7w–ab** in moderate to excellent yields. Notably, stoichiometric amount of Shimada catalyst provides only slight trace of the desired compound **7v** with pivaloyl chloride. In addition, some functionalities were successfully introduced, such as methoxy **7ad**, chloride **7ag**, or terminal alkyne **7ah**. Noteworthy, this latter represents a unique platform for introduction of various triazole moiety through copper(I)-catalyzed alkyne-azide cycloaddition (CuAAC). Gratifyingly, dinuclear copper catalyst **21** developed by Straub et al.⁵⁸ allowed the formation of derivatives **7ai** in excellent yield. Finally, in order to study the impact of other functional groups on the biological activity, further electrophiles such as carbamoyl chloride, chloroformate, and tosylate were tested under our optimized conditions. Unfortunately, all attempts were found to be unproductive.

Biological evaluation of C3''-acylated fidaxomicin derivatives. The biological activities for these 30 fidaxomicin analogs were evaluated by determination of the minimum inhibitory

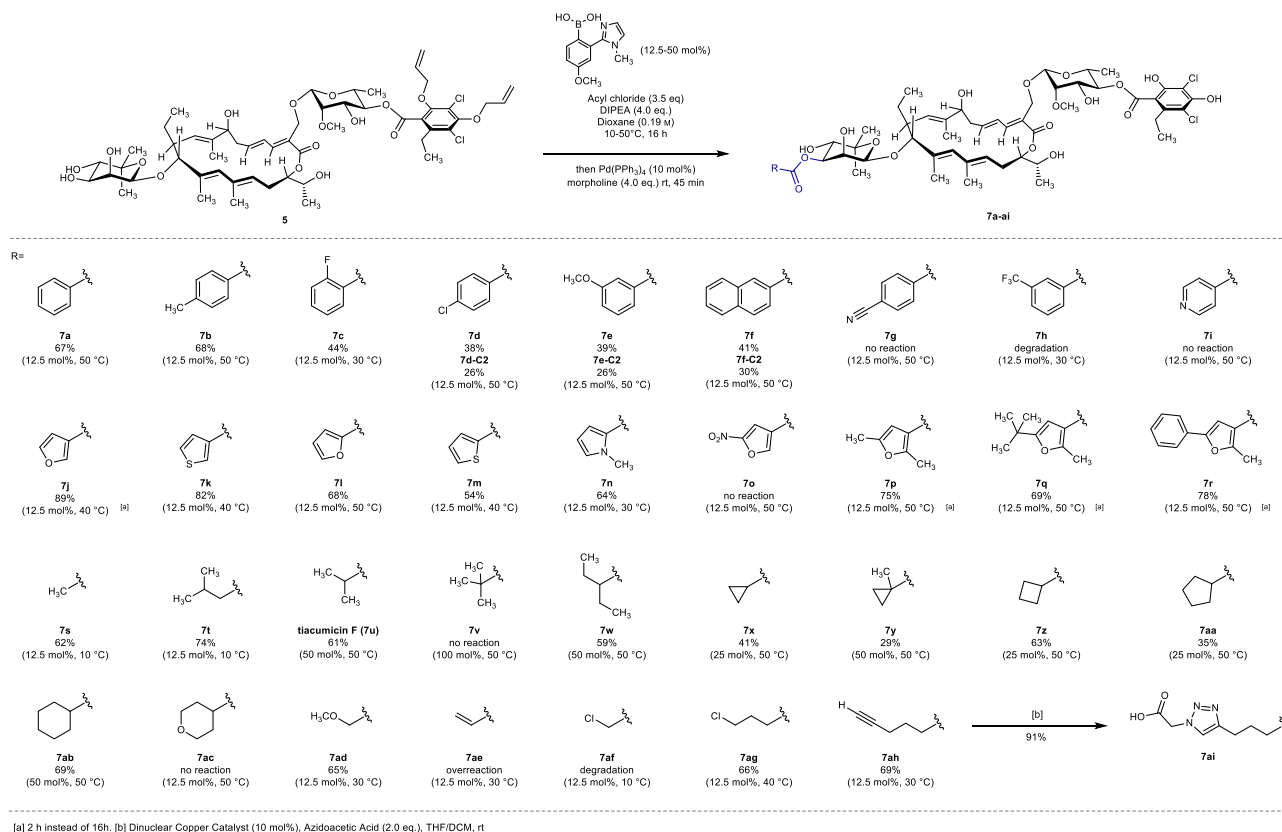


Fig. 7 Scope of selective C3'-functionalization of 5. Acylation of **5** applying the optimized catalyst system with various acyl chlorides.

	1	4	7a	7b	7c	7d	7d-C2	7e	7e-C2	7f	7f-C2	7j	7k	7l	7m	7n
C. difficile^a																
ATCC 43255	0.03	0.5	0.25	0.5	0.5	0.5	2	0.5	1	0.5	1	0.12	0.25	0.5	0.25	0.12
ATCC 700057	≤0.015-0.03	0.5	0.25	0.25	0.5	1	2	0.25	0.5	0.5	2	0.06	0.25	0.25	0.25	0.06
ATCC BAA-1805 ^b	0.06-0.12	1	0.5	1	1	2	8	1	4	2	8	0.5	0.5	1	0.5	0.25
ATCC BAA-1875 ^b	0.03	1	0.5	1	1	1	4	0.5	2	1	4	0.25	0.5	1	0.5	0.25
ATCC 9689 (RT 001)	≤0.015	0.12	0.12	0.25	0.12	0.5	1	0.25	0.5	0.5	2	0.03	0.12	0.12	0.12	0.06
MMX 8260 (RT 017)	0.03-0.06	1	0.25	0.5	1	1	4	0.5	1	0.25	4	0.12	0.25	0.5	0.25	0.12
MMX 8282 (RT 017)	≤0.015-0.03	1	0.25	0.25	0.25	1	2	0.12	1	0.25	2	0.25	0.25	0.12	0.25	0.12
MMX 5680 (RT 027)	0.06	2	0.5	1	2	2	4	1	2	2	16	0.25	1	1	1	0.5
MMX 8264 (RT 027)	0.03-0.12	2	0.25	0.5	1	2	8	0.5	1	1	8	0.5	0.25	0.5	0.5	0.12
MMX 8290 (RT 078)	0.03	2	0.5	1	1	2	4	0.5	2	1	16	0.25	0.5	0.5	0.5	0.25
M. tuberculosis^c																
	0.25	4	4-8	4	4	8	8-16	4	4	8	16-32	0.5	1-2	2	2	2
	7p	7q	7r	7s	7t	7u	7w	7x	7y	7z	7aa	7ab	7ad	7ag	7ah	7ai
C. difficile^a																
ATCC 43255	0.25	4	2	0.5	0.25	0.06	0.12	0.12	0.12	0.12	0.25	0.5	2	0.5	0.25	>16
ATCC 700057	0.25	8	8	0.25	0.25	0.06	0.06	0.03	0.12	0.25	0.5	1	0.5	0.25	0.25	>16
ATCC BAA-1805 ^b	0.25	>16	16	1	1	0.25	0.25	0.25	0.5	0.5	1	2	4	0.5	0.5	>16
ATCC BAA-1875 ^b	0.5	16	4	1	0.25	0.12	0.25	0.12	0.25	0.5	0.5	1	2	0.5	0.5	>16
ATCC 9689 (RT 001)	0.12	4	1	0.06	0.06	≤0.015	0.03	0.03	0.03	0.06	0.12	0.25	0.25	0.12	0.03	8
MMX 8260 (RT 017)	0.25	4	4	0.5	0.25	0.06	0.06	0.12	0.12	0.25	0.25	0.5	1	0.25	0.12	>16
MMX 8282 (RT 017)	0.25	8	4	0.25	0.12	0.12	0.25	0.12	0.25	0.25	0.5	0.5	1	0.25	0.12	>16
MMX 5680 (RT 027)	0.5	>16	>16	1	1	0.25	0.25	0.5	0.5	0.5	1	2	4	1	0.5	>16
MMX 8264 (RT 027)	0.5	>16	16	2	1	0.06	0.12	0.5	0.5	0.25	1	2	4	0.5	0.5	>16
MMX 8290 (RT 078)	0.5	16	4	0.5	0.25	0.12	0.25	0.12	0.25	0.25	0.5	1	2	0.5	0.25	>16
M. tuberculosis^c																
	8	16-32	>64	0.5-1	1-2	0.25-0.5	1-2	0.5-1	4	2	1-2	4	1-2	2	1-2	>16

^a MIC₉₀ determined by broth microdilution assay^{59,60}; ^b toxigenic; ^c MIC₉₀ determined on a GFP-expressing *M. tuberculosis* strain.⁶¹

Fig. 8 Minimum inhibitory concentrations (MIC) values. Determination of the MIC in µg/mL against a panel of different *C. difficile* strains and *M. tuberculosis*. RT Ribotype.

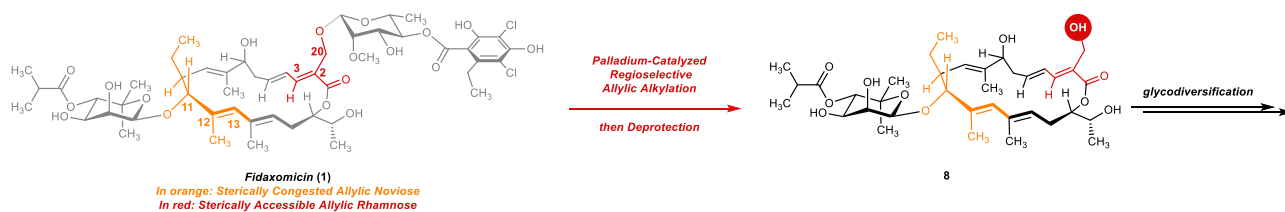


Fig. 9 Site-selective allylic functionalization of (1). Overview of the strategy.

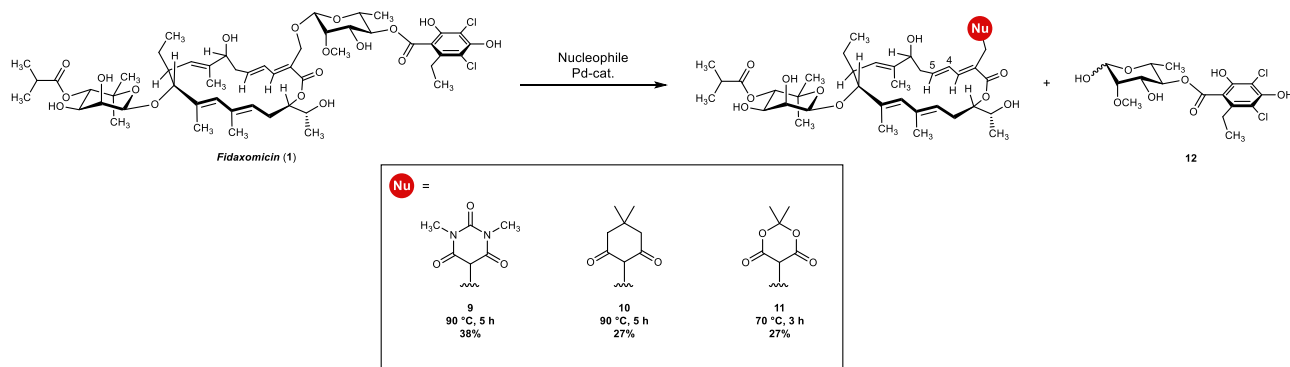


Fig. 10 Allylic substitution of the rhamnose-resorcylate moiety. Scope of the site-selective allylic functionalization of (1).

concentration (MIC) and are summarized in Fig. 8. The MIC values for *C. difficile* were determined using the broth micro-dilution assay and determination of bacterial growth by observation of turbidity (MIC₉₀)^{59,60}. The values against *M. tuberculosis* were evaluated using a recently developed method on a GFP-expressing *M. tuberculosis* strain and observation of growth by fluorescence⁶¹. A fluorescence reduction of 90% as compared to the no-drug control was reported as MIC₉₀ (for details see Supplementary Information, section Determination of the minimum inhibitory concentration). All compounds were evaluated against *M. tuberculosis* as well as ten *C. difficile* isolates. As expected with previously reported data, OP1118 (4) displayed reduced antibacterial activity, pointing out the pivotal role of the isobutyric ester moiety for the bioactivity. Intriguingly, aromatic derivatives 7a–7f showed similar bioactivities than for OP1118 (4). Interestingly, C2^{''}-benzoylated derivatives 7d–f–C2 were found to be less active than the C3^{''}-benzoylated analogs that supports hypotheses drawn from the cryo-EM structural analysis. To our delight, heteroaromatic derivatives 7j–n were found to have good bioactivity for all the tested bacterial strains compared to the aromatic series 7a to 7f–C2. Noteworthy, derivative 7j is highly active against *M. tuberculosis* (MIC = 0.5 µg/mL) as well as the *C. difficile* strains; therefore, the latter represents an excellent landmark for implementation of substitution on the furan moiety. Unfortunately, first decorated versions 7p–r of the more potent heteroaromatic derivative 7j were found to be less active, such as the derivatives 7q–r, which are sterically more demanding. Nevertheless, this first batch of substituted furan derivatives indicated that smaller functional groups and/or functionalizations at the position 4 of the furan should be considered in the future for the modification of derivative 7r. On the other hand, considering the reported bioactivities of tiacumicin F (7u), non-aromatic C3^{''}-acylated fidaxomicin derivatives were expected to have similar or improved bioactivities. Indeed, fidaxomicin analogs 7s–ah were found to have good bioactivity, and especially, derivatives 7w–x. Whereas derivatives 7j, 7u, and 7x have excellent bioactivities against all tested bacterial strains, these are slightly less potent than fidaxomicin itself. Nevertheless, this study validates our hypothesis and a fine-tuning of those

derivatives may pave the way to discover more potent antibiotic derivatives.

Allylic substitution of the rhamnose-resorcylate moiety. Over the past 50 years, metal-catalyzed allylic (asymmetric) substitution emerged as an extremely appealing and efficient tool to form C–C and C–heteroatom bonds with applications in target-oriented synthesis of natural products and active pharmaceutical ingredients⁶². Whereas numerous developments allow the use of a broad range of allylic substrates, the use of allylic acetals as allyl donors remains scarce and were used as carbon sources in palladium-catalyzed umpolung allylations^{63,64}. Nonetheless, these reports led us to consider the allylic noviose and the allylic rhamnose of fidaxomicin as potential electrophilic partner in metal-catalyzed allylic substitution. Considering the steric congestion around the allylic noviose moiety as well as the electronically favored environment around the rhamnose due to the proximity to the conjugated macrolactone, we envisioned that discrimination of the allylic rhamnose versus allylic noviose would be possible. Moreover, using an appropriate oxygen nucleophile would lead, after deprotection, to 8 that represents a unique platform for glycodiversification (Fig. 9).

Unfortunately, extensive screening with differently protected O-nucleophiles remained unsuccessful as either no conversion or complex mixtures were obtained. This prompted us to consider other types of nucleophiles. To our delight, we were pleased to find that C-nucleophiles were competent, thus validating our strategy (Fig. 10). Cyclic 1,3-dicarbonyls, such as 9, 10, and 11 were synthesized with concomitant isomerization of the diene moiety (between C4 and C5), which is in line with the ability of palladium to migrate along a π system⁶⁵. Whereas substitution with *N,N*-dimethyl barbituric acid and dimedone required temperatures of 90 °C, the reaction with Meldrum's acid led to decomposition; however, lowering the temperature to 70 °C was beneficial to provide the desired product 11 in 27% yield. Unfortunately, extensive screening of the parameters of the reaction with special emphasis on phosphine ligand did not improve the reaction further and isomerization of the double bond could not be prevented. Noteworthy, we ruled out a

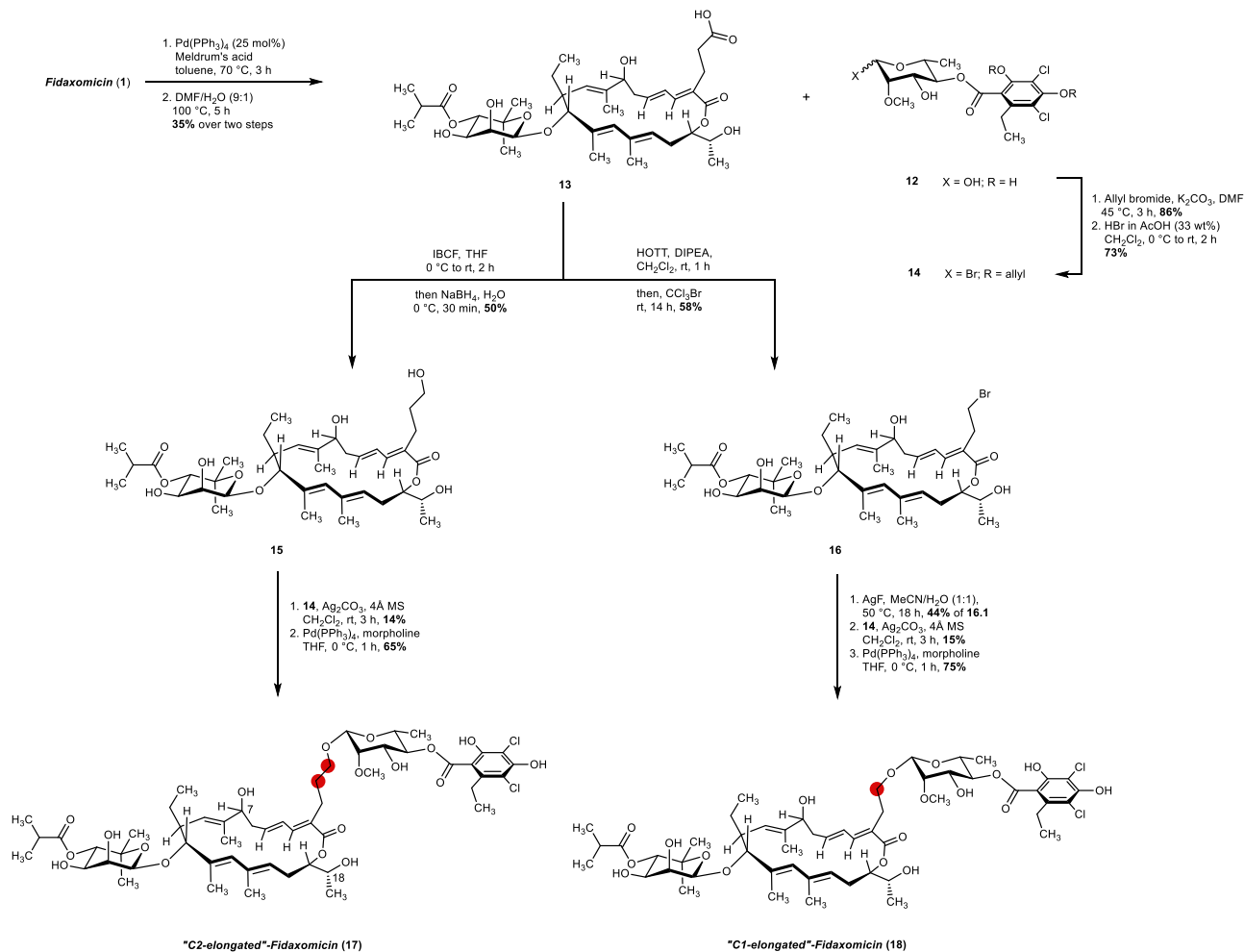


Fig. 11 Synthesis of C2- and C1-elongated fidaxomicin analogs. Detailed synthetic route toward C2- and C1-elongated fidaxomicin analogs **17** and **18**. IBCF Isobutyl chloroformate, HOTT S-(1-oxido-2-pyridinyl)-1,1,3,3-tetramethylthiuronium hexafluorophosphate.

plausible Baylis–Hillman type mechanism by control experiments (see Supplementary Information, section Experimental procedures Tsuji–Trost functionalizations).

Therefore, to best of our knowledge, this transformation represents a unique palladium-catalyzed allylic substitution with such a complex electrophilic partner. Moreover, given the abundance of allylic glycoside derivatives in biologically active natural products (especially in polyene macrolides), we believe that this finding will pave the way for further development in drug discovery⁶⁶. Next, we decided to take advantage of the Meldrum's acid derivative **11**. Upon hydrolysis and decarboxylation of the Meldrum's acid moiety, carboxylic acid **13** was obtained in 35% yield over two steps (Fig. 11). Usually, Meldrum's acid **11** was directly submitted to hydrolysis without further purification due to the difficult separation of **11** from its *E*, *Z*-isomer, which is formed in 12% yield as a by-product of the Tsuji–Trost reaction. The carboxylic acid **13** acts as suitable functional group for a great variety of transformations such as esterification/amide coupling, reduction, Curtius rearrangement, or decarboxylative brominations and consequently allowing the synthesis of analogs with one or two additional CH₂-groups, which are difficult or not even possible to obtain by fermentation of a genetically modified producer strain.

As we were able to regain high quantities of the cleaved rhamnose-orsellinate moiety **12** after the Tsuji–Trost reaction, we prepared C2- and C1-elongated fidaxomicin analogs, starting from fidaxomicin (**1**). Therefore, we addressed the selective

reduction of the carboxylic acid **13** next. Upon screening of several conditions, we found that formation of the mixed anhydride using isobutyl chloroformate and subsequent reduction with NaBH₄ yields the desired alcohol **15**, besides some traces of competing isobutyl ester cleavage on the noviose part⁶⁷.

Transformation of the rhamnosyl-orsellinate **12** into a suitable glycosyl donor was achieved via allyl protection of the phenolic hydroxy groups, followed by substitution of the anomeric hydroxy group by bromide using HBr to give glycosyl bromide **14** as a single anomer. With glycosyl bromide **14** and alcohol **15** in hands, we performed the glycosylation using Königs–Knorr conditions⁶⁸ that gave after allyl deprotection, the desired C2-elongated fidaxomicin **17**. Besides glycosylation on the primary alcohol, minor amounts of glycosylation at C7- and C18 hydroxy groups were observed as well, which accounts for the relatively low yield. The desired C2-elongated fidaxomicin **17** was surprisingly obtained as a single anomer. NOESY spectra as well as similar ¹J_{CH} coupling constants (1: ¹J_{CH} = 155 Hz, 17: ¹J_{CH} = 157 Hz) indicate that most probably β-glycosylation occurred^{69,70}. NOESY analysis of the glycosyl bromide **14**, however, revealed that the α-anomer was obtained as the major isomer, indicating an S_N2-type mechanism (see Supplementary Figs. 1, 88, 100, and 101)

Furthermore, we investigated decarboxylative brominations via a Barton ester to give bromide **16**. Best yields were achieved when Barton ester formation was performed using the coupling reagent HOTT^{71–73} directly followed by addition of

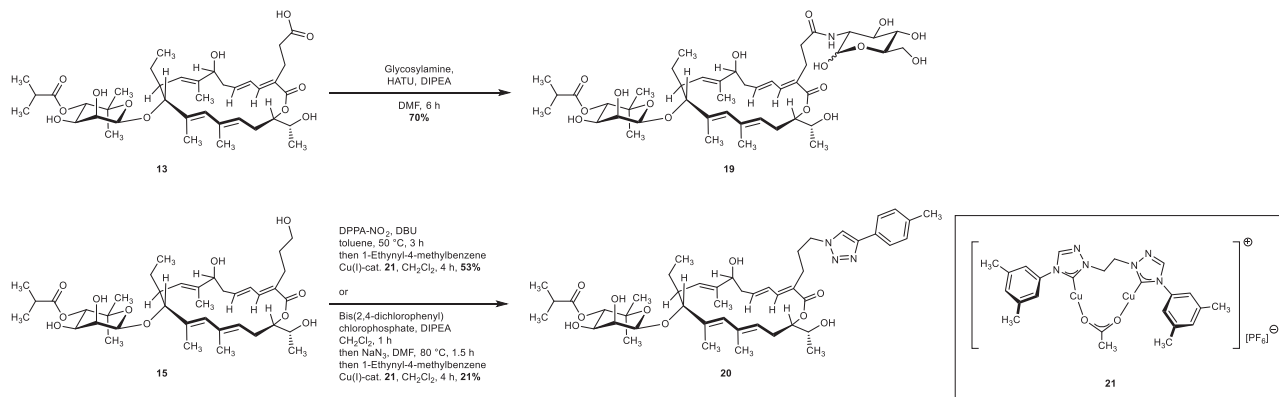


Fig. 12 Functionalization of C2-elongated carboxylic acid 13 and alcohol 15. Synthesis of glucosamide-fidaxomicin **19** and triazole **20**. HATU 1-[Bis(dimethylamino)methylene]-1H-1,2,3-triazolo[4,5-b]pyridinium 3-oxide hexafluorophosphate, DPPA-NO₂Di-(nitrophenyl)phosphoryl azide.

bromotrichloromethane⁷⁴. The following hydrolysis of bromide **16** was found to be troublesome⁷⁵. Various by-products that originate from transesterifications on the macrolactone were observed and made purification difficult. Upon optimization, yields of up to 44% of the desired alcohol were obtained. Final glycosylation reaction, which had to be warmed to 40 °C in order to get complete conversion, and allyl deprotection then yielded the C1-elongated fidaxomicin **18**.

As already outlined before, the carboxylic acid **13** as well as the alcohol **15** and **16.1** can serve as a platform for further modifications. As we are interested in the role of the sugar moieties on fidaxomicin, we investigated displacement by other sugar moieties on this stage. As a suitable carbohydrate, we choose glycosylamine, which could be coupled to the carboxylic acid moiety using HATU to afford the desired glycosylamide **19** in high yields (Fig. 12). On the other hand, we envisioned to introduce 1,2,3-triazole scaffolds, which are relatively stable to hydrolytic conditions, metabolic degradation, and redox conditions. Moreover, they are known to be bioisosteres of numerous functional groups and they are prone to H-bonds and π - π stackings interactions. All these features rendering 1,2,3-triazole ring highly attractive to access lead compounds in medicinal chemistry^{76–78}. Whereas activation of the alcohol **15** through sulfonate formation followed by sodium azide displacement was unselective, we found out that the one-pot azidation of alcohol **15** using bis(*p*-nitrophenyl) phosphorazidate was highly selective for the primary alcohol⁷⁹. Subsequent Cu-mediated cycloaddition delivered the triazole **20** in good overall yield. Unfortunately, reproducibility issues with the azidation step prompt us to consider another sequence. After optimization, the alcohol **15** was fully converted to the desired phosphate using bis-(2,4-dichlorophenyl) chlorophosphate. Upon S_N2-type mechanism with sodium azide followed by previously used CuAAC with 1-ethynyl-4-methylbenzene, the triazole **20** was obtained in an acceptable yield. Gratifyingly, due to the highly selective activation of the primary alcohol of **15**, this strategy would allow us to obtain an expeditious library of C2-elongated fidaxomicin analogs via S_N2-type mechanism by varying the nucleophile.

Biological evaluation of rhamnose-edited fidaxomicin derivatives. The biological activities for these compounds bearing variations on the rhamnose-homoorsellinate part are summarized in Fig. 13. While fidaxomicin (**1**) is highly active against *M. tuberculosis* (MIC = 0.25 μ g/mL) and *C. difficile*, the activity for the C1- and C2-elongated derivatives gradually drops, thereby indicating that binding to the RNAP is diminished probably due

to a reduced interaction of the rhamnose sugar with Arg89. Therefore, we conclude that the position of the rhamnose-resorcyate moiety is crucial for the excellent activity of fidaxomicin (**1**) due to optimal interactions with amino acid residues in the binding pocket.

Interestingly, derivatives **11** and **19**, where the rhamnose moiety is exchanged by Meldrum's acid and glycosylamine, respectively, are still active against *M. tuberculosis*, even though the activity significantly decreased. However, activity against *C. difficile* was lost. To our delight, triazole **20**, whose structure considerably differs from fidaxomicin, still features good activity against *M. tuberculosis*.

Conclusion

In conclusion, we achieved the synthesis of a variety of novel fidaxomicin derivatives based on structural information provided by cryo-EM structures of fidaxomicin binding to the target bacterial RNAP. A highly site-selective method for the acylation of the noviose moiety using Shimada's catalyst gave access to 30 novel fidaxomicin analogs with modifications on the 3''-OH group. These derivatives showed similar antibacterial activities compared to natural product **1** and thereby confirming our hypothesis that modifications in these positions are beneficial in retaining activity. In addition, our search for new reactions regarding fidaxomicin resulted in the development of a Tsuji–Trost type allylic substitution with cyclic 1,3-diketones to furnish rhamnose-resorcyate cleavage and thereby giving access to carboxylic acid **13** that would serve as a basis for a variety of glycodiversifications such as **19**. Furthermore, triazole **20** retained some antibacterial activity and therefore use of these azide precursors represents a promising platform for further derivatizations. At present, this Tsuji–Trost approach is limited to C-nucleophiles, but investigations to broaden the scope of this reaction are currently under investigation and will be reported in due course. Applying this reaction, C1- and C2-elongated fidaxomicin analogs **17** and **18** were synthesized, thus representing the first examples of a complex, multi-step modification of natural antibiotic fidaxomicin (**1**). These new fidaxomicin derivatives and further derivatives prepared by the methods described in this work may prove to be promising, future candidates for the treatment of bacterial infections and may contribute to ongoing efforts to reduce rate of resistance development.

Methods

Full methods and data are given in the Supplementary Material, see Supplementary Methods section.

	1	18	17	11	19	20
C. difficile^a						
ATCC 43255	0.03	0.5	2	>16	>16	4
ATCC 700057	≤0.015-0.03	0.5	4	>16	>16	8
ATCC BAA-1805 ^b	0.06-0.12	0.5	8	>16	>16	8
ATCC BAA-1875 ^b	0.03	1	4	>16	>16	8
ATCC 9689 (RT 001)	≤0.015	0.06	1	>16	>16	2
MMX 8260 (RT 017)	0.03-0.06	0.12	4	>16	>16	2
MMX 8282 (RT 017)	≤0.015-0.03	0.12	2	>16	>16	4
MMX 5680 (RT 027)	0.06	1	8	>16	>16	16
MMX 8264 (RT 027)	0.03-0.12	1	8	>16	>16	8
MMX 8290 (RT 078)	0.03	0.5	4	>16	>16	8
M. tuberculosis^c						
	0.25	2-4	8	8	8-16	2-4

^a MIC₉₀ determined by broth microdilution assay^{59,60}; ^b toxigenic; ^c MIC₉₀ determined on a GFP-expressing *M. tuberculosis* strain.⁶¹

Fig. 13 Minimum inhibitory concentration (MIC) values. Determination of the MIC in µg/mL against a panel of different *C. difficile* strains and *M. tuberculosis*. RT Ribotype.

Reporting summary. Further information on research design is available in the Nature Research Reporting Summary linked to this article.

Data availability

Compounds and the corresponding biological data were deposited at PubChem and PubChem BioAssay (SID 440785998–440786033). Procedures and analytical data, including NMR spectra, are available in the Supplementary Information or can be requested from the corresponding author.

Received: 21 December 2020; Accepted: 31 March 2021;

Published online: 10 May 2021

References

- Parenti, F., Pagani, H. & Beretta, G. Lipiarmycin, A. New antibiotic from *Actinoplanes* I. Description of the producer strain and fermentation studies. *J. Antibiot.* **28**, 247–252 (1975).
- Coronelli, C., White, R. J., Lancini, G. C. & Parenti, F. Lipiarmycin, A. New antibiotic from *Actinoplanes* II. Isolation, chemical, biological and biochemical characterization. *J. Antibiot.* **28**, 253–259 (1975).
- Omura, S. et al. Clostomicins, new antibiotics produced by *Micromonospora echinospora* subsp. *Armeniaca* subsp. nov. I. Production, isolation, and physico-chemical and biological properties. *J. Antibiot.* **39**, 1407–1412 (1986).
- Takashi, Y., Iwai, Y. & Omura, S. Clostomicins, new antibiotics produced by *Micromonospora echinospora* subsp. *Armeniaca* subsp. nov. II. Taxonomic study of the producing microorganism. *J. Antibiot.* **39**, 1413–1418 (1986).
- Theriault, R. J. et al. Tiacumicins, a novel complex of 18-membered macrolide antibiotics I. Taxonomy, fermentation and antibacterial activity. *J. Antibiot.* **40**, 567–574 (1987).
- Hochlowski, J. E. et al. Tiacumicins, a novel complex of 18-membered macrolides II. Isolation and structure determination. *J. Antibiot.* **40**, 575–588 (1987).
- Kurabachew, M. et al. Lipiarmycin targets RNA polymerase and has good activity against multidrug-resistant strains of *Mycobacterium tuberculosis*. *J. Antimicrob. Chemother.* **62**, 713–719 (2008).
- McAlpine, J. B., Jackson, M. & Karwowski, J. Tiacumicin compounds. US 4,918,174 (1990).
- Biedenbach, D. J., Ross, J. E., Putnam, S. D. & Jones, R. N. In vitro activity of fidaxomicin (OPT-80) tested against contemporary clinical isolates of *Staphylococcus* spp. and *Enterococcus* spp. *Antimicrob. Agents Chemother.* **54**, 2273–2275 (2010).
- Gerber, M. & Ackermann, G. OPT-80, a macrocyclic antimicrobial agent for the treatment of *Clostridium difficile* infections: a review. *Expert Opin. Investig. Drugs* **17**, 547–553 (2008).
- Babakhani, F., Gomez, A., Robert, N. & Sears, P. Killing kinetics of fidaxomicin and its major metabolite, OP-1118, against *Clostridium difficile*. *J. Med. Microbiol.* **60**, 1213–1217 (2011).
- Miller, M. Fidaxomicin (OPT-80) for the treatment of *Clostridium difficile* infection. *Expert Opin. Pharmacother.* **11**, 1569–1578 (2010).
- European Medicines Agency. *Assessment Report Difclir.* (2011).
- Erb, W. & Zhu, J. From natural product to marketed drug: the tiacumicin odyssey. *Nat. Prod. Rep.* **30**, 161–174 (2013).
- McAlpine, J. B. The ups and downs of drug discovery: the early history of fidaxomicin. *J. Antibiot.* **70**, 492–494 (2017).
- Dorst, A., Jung, E. & Gademann, K. Recent advances in mode of action and biosynthesis studies of the clinically used antibiotic fidaxomicin. *Chimia* **74**, 270–273 (2020).
- Dorst, A. & Gademann, K. Chemistry and biology of the clinically used macrolactone antibiotic fidaxomicin. *Helv. Chim. Acta* **103**, e2000038 (2020).
- Lin, W. et al. Structural basis of transcription inhibition by fidaxomicin (lipiarmycin A3). *Mol. Cell* **70**, 60–71 (2018).
- Boyaci, H. et al. Fidaxomicin jams *Mycobacterium tuberculosis* RNA polymerase motions needed for initiation via RbpA contacts. *Elife* **7**, e34823 (2018).
- Morichaud, Z., Chaloin, L. & Brodolin, K. Regions 1.2 and 3.2 of the RNA polymerase σ subunit promote DNA melting and attenuate action of the antibiotic lipiarmycin. *J. Mol. Biol.* **428**, 463–476 (2016).
- Wright, P. M., Seiple, I. B. & Myers, A. G. The evolving role of chemical synthesis in antibacterial drug discovery. *Angew. Chem. Int. Ed.* **53**, 8840–8869 (2014).
- World Health Organization (WHO). *Global Tuberculosis Report 2020*.
- Andries, K. et al. A diarylquinoline drug active on the ATP synthase of *Mycobacterium tuberculosis*. *Science* **307**, 223–227 (2005).
- Conradie, F. et al. Treatment of highly drug-resistant pulmonary tuberculosis. *N. Engl. J. Med.* **382**, 893–902 (2020).
- Bloemberg, G. V., Gagneux, S. & Böttger, E. C. Acquired resistance to bedaquiline and delamanid in therapy for tuberculosis. *N. Engl. J. Med.* **373**, 1986–1988 (2015).
- Thorpe, C. M. et al. U.S.-based national surveillance for fidaxomicin susceptibility of *Clostridioides difficile*-associated diarrheal isolates from 2013 to 2016. *Antimicrob. Agents Chemother.* **63**, e00391–19 (2019).
- Freeman, J. et al. Five-year Pan-European, longitudinal surveillance of *Clostridium difficile* ribotype prevalence and antimicrobial resistance: the extended ClosER study. *Eur. J. Clin. Microbiol. Infect. Dis.* **39**, 169–177 (2020).
- McAlpine, J. E. & Hochlowski, J. E. Diallyltiacumicin compounds. US 5,583,115 (1996).
- Wu, M.-C., Huang, C.-C., Lu, Y.-C. & Fan, W.-J. Derivatives of tiacumicin B as anti-cancer agents. US 2009/0110718 A1 (2008).
- Xiao, Y. et al. Characterization of tiacumicin B biosynthetic gene cluster affording diversified tiacumicin analogues and revealing a tailoring dihalogenase. *J. Am. Chem. Soc.* **133**, 1092–1105 (2011).
- Niu, S. et al. Characterization of a sugar-O-methyltransferase TiaS5 affords new tiacumicin analogues with improved antibacterial properties and reveals substrate promiscuity. *ChemBioChem* **12**, 1740–1748 (2011).
- Zhang, H. et al. Tiacumicin congeners with improved antibacterial activity from a halogenase-inactivated mutant. *J. Nat. Prod.* **81**, 1219–1224 (2018).

33. Yu, Z. et al. Characterizing two cytochrome P450s in tiacumicin biosynthesis reveals reaction timing for tailoring modifications. *Org. Lett.* **21**, 7679–7683 (2019).
34. Dorst, A., Shchelik, I. S., Schäfle, D., Sander, P. & Gademann, K. Synthesis and biological evaluation of iodinated fidaxomicin antibiotics. *Helv. Chim. Acta* **103**, e2000130 (2020).
35. Dorst, A. et al. Semisynthetic analogs of the antibiotic fidaxomicin—design, synthesis, and biological evaluation. *ACS Med. Chem. Lett.* **11**, 2414–2420 (2020).
36. Shue, Y.-K. et al. Tiacumicin compounds. US 7,507,564 B2 (2003).
37. Křen, V. & Řezanka, T. Sweet antibiotics—the role of glycosidic residues in antibiotic and antitumor activity and their randomization. *FEMS Microbiol. Rev.* **32**, 858–889 (2008).
38. Jamison, M. T. Mangrolide A. A Novel Marine Derived Polyketide with Selective Antibiotic Activity. PhD Thesis, University of Texas Southwestern Medical Center at Dallas. (2013).
39. DeBrabander, J. Small molecule compounds selective against Gram-negative bacterial infections. WO 2015/175695 A1 (2015).
40. Hattori, H. et al. Total synthesis and biological evaluation of the glycosylated macrocyclic antibiotic mangrolide A. *Angew. Chem. Int. Ed.* **57**, 11020–11024 (2018).
41. Hattori, H., Hoff, L. V. & Gademann, K. Total synthesis and structural revision of mangrolide D. *Org. Lett.* **21**, 3456–3459 (2019).
42. Gong, J., Li, W., Fu, P., Macmillan, J. & De Brabander, J. K. Isolation, structure, and total synthesis of the marine macrolide mangrolide D. *Org. Lett.* **21**, 2957–2961 (2019).
43. Kaufmann, E., Hattori, H., Miyatake-Onozabal, H. & Gademann, K. Total synthesis of the glycosylated macrolide antibiotic fidaxomicin. *Org. Lett.* **17**, 3514–3517 (2015).
44. Norsikian, S. et al. Total synthesis of tiacumicin B: implementing H-bond-directed acceptor delivery for highly selective β -glycosylations. *Angew. Chem. Int. Ed.* **59**, 6612–6616 (2020).
45. Kawabata, T. *Site-Selective Catalysis*. (Springer International Publishing, 2016).
46. Robles, O. & Romo, D. Chemo- and site-selective derivatizations of natural products enabling biological studies. *Nat. Prod. Rep.* **31**, 318–334 (2014).
47. Ichikawa, Y., Chiu, Y.-H., Shue, Y.-K. & Babakhani, F. K. Antibiotic macrocycle compounds and methods of manufacture and use thereof. US 8,044,030 B2 (2008).
48. Anderson, A. C. The process of structure-based drug design. *Chem. Biol.* **10**, 787–797 (2003).
49. Wong, S. E. & Lightstone, F. C. Accounting for water molecules in drug design. *Expert Opin. Drug Disco.* **6**, 65–74 (2011).
50. Spyraakis, F. et al. The roles of water in the protein matrix: a largely untapped resource for drug discovery. *J. Med. Chem.* **60**, 6781–6827 (2017).
51. Hattori, H., Kaufmann, E., Miyatake-Onozabal, H., Berg, R. & Gademann, K. Total synthesis of tiacumicin A. Total synthesis, relay synthesis, and degradation studies of fidaxomicin (tiacumicin B, lipiarmycin A3). *J. Org. Chem.* **83**, 7180–7205 (2018).
52. González-Sabín, J., Morán-Ramallal, R. & Rebolledo, F. Regioselective enzymatic acylation of complex natural products: expanding molecular diversity. *Chem. Soc. Rev.* **40**, 5321–5335 (2011).
53. Dimakos, V. & Taylor, M. S. Site-selective functionalization of hydroxyl groups in carbohydrate derivatives. *Chem. Rev.* **118**, 11457–11517 (2018).
54. Taylor, M. S. Catalysis based on reversible covalent interactions of organoboron compounds. *Acc. Chem. Res.* **48**, 295–305 (2015).
55. Beale, T. M. & Taylor, M. S. Synthesis of cardiac glycoside analogs by catalyst-controlled, regioselective glycosylation of digitoxin. *Org. Lett.* **15**, 1358–1361 (2013).
56. Lee, D. & Taylor, M. S. Boronic acid-catalyzed regioselective acylation of carbohydrate derivatives. *J. Am. Chem. Soc.* **133**, 3724–3727 (2011).
57. Shimada, N., Nakamura, Y., Ochiai, T. & Makino, K. Catalytic activation of cis-vicinal diols by boronic acids: site-selective acylation of carbohydrates. *Org. Lett.* **21**, 3789–3794 (2019).
58. Berg, R. et al. Highly active dinuclear copper catalysts for homogeneous azide-alkyne cycloadditions. *Adv. Synth. Catal.* **354**, 3445–3450 (2012).
59. Clinical and Laboratory Standards Institute (CLSI). *Performance Standards for Antimicrobial Susceptibility Testing* 29th edn (Clinical and Laboratory Standards Institute, 2019).
60. Clinical and Laboratory Standards Institute (CLSI). *Methods for Antimicrobial Susceptibility Testing of Anaerobic Bacteria*. 9th edn (Clinical and Laboratory Standards Institute, 2018).
61. Dal Molin, M. et al. Identification of novel scaffolds targeting *Mycobacterium tuberculosis*. *J. Mol. Med.* **97**, 1601–1613 (2019).
62. Trost, B. M. & Crawley, M. L. *Enantioselective Allylic Substitutions in Natural Product Synthesis BT – Transition Metal Catalyzed Enantioselective Allylic Substitution in Organic Synthesis*. (ed. Kazmaier, U.) 321–340 (Springer Berlin Heidelberg, 2012).
63. Kimura, M., Shimizu, M., Shibata, K., Tazoe, M. & Tamaru, Y. Pd-catalyzed nucleophilic alkylation of aliphatic aldehydes with allyl alcohols: allyl, 2-tetrahydrofuryl, and 2-tetrahydropyranyl ethers as useful C3, C4, and C5 sources. *Angew. Chem. Int. Ed.* **42**, 3392–3395 (2003).
64. Shimizu, M., Kimura, M. & Tamaru, Y. Use of allyl, 2-tetrahydrofuryl, and 2-tetrahydropyranyl ethers as useful C3-, C4-, and C5-carbon sources: palladium-catalyzed allylation of aldehydes. *Chem. A Eur. J.* **11**, 6629–6642 (2005).
65. Trost, B. M., Urch, C. J. & Hung, M.-H. Regiochemical directing effects in palladium catalyzed alkylations with polyene electrophilic partners. *Tetrahedron Lett.* **27**, 4949–4952 (1986).
66. Elshahawi, S. I., Shaaban, K. A., Kharel, M. K. & Thorson, J. S. A comprehensive review of glycosylated bacterial natural products. *Chem. Soc. Rev.* **44**, 7591–7697 (2015).
67. Soai, K., Yokoyama, S. & Mochida, K. Reduction of symmetric and mixed anhydrides of carboxylic acids by sodium borohydride with dropwise addition of methanol. *Synthesis* **7**, 647–648 (1987).
68. Koenigs, W. & Knorr, E. Über einige Derivate des Traubenzuckers und der Galactose. *Chem. Ber.* **34**, 957–981 (1901).
69. Crich, D. & Picione, J. Direct synthesis of the β -L-rhamnopyranosides. *Org. Lett.* **5**, 781–784 (2003).
70. Bock, K. & Pedersen, C. A study of ^{13}C coupling constants in hexopyranoses. *J. Chem. Soc. Perkin Trans. 2*, 293–297 (1974).
71. Garner, P., Anderson, J. T. & Dey, S. S-(1-Oxido-2-pyridinyl)-1,1,3,3-tetramethyl-thiuronium hexafluorophosphate. A new reagent for preparing hindered barton esters. *J. Org. Chem.* **63**, 5732–5733 (1998).
72. Bailén, M. A., Chinchilla, R., Dodsworth, D. J. & Nájera, C. 2-Mercaptopyrindone 1-oxide-based uronium salts: new peptide coupling reagents. *J. Org. Chem.* **64**, 8936–8939 (1999).
73. Albericio, F., Bailén, M. A., Chinchilla, R., Dodsworth, D. J. & Nájera, C. 2-Mercaptopyrindone-1-oxide-based peptide coupling reagents. *Tetrahedron* **57**, 9607–9613 (2001).
74. Barton, D. H. R., Crich, D. & Motherwell, W. B. A practical alternative to the Hunsdiecker reaction. *Tetrahedron Lett.* **24**, 4979–4982 (1983).
75. Renata, H. et al. Development of a concise synthesis of ouabagenin and hydroxylated corticosteroid analogues. *J. Am. Chem. Soc.* **137**, 1330–1340 (2015).
76. Bonandi, E. et al. The 1,2,3-triazole ring as a bioisostere in medicinal chemistry. *Drug Discov. Today* **22**, 1572–1581 (2017).
77. Dheer, D., Singh, V. & Shankar, R. Medicinal attributes of 1,2,3-triazoles: current developments. *Bioorg. Chem.* **71**, 30–54 (2017).
78. Bozorov, K., Zhao, J. & Aisa, H. A. 1,2,3-Triazole-containing hybrids as leads in medicinal chemistry: a recent overview. *Bioorg. Med. Chem.* **27**, 3511–3531 (2019).
79. Mizuno, M., Shioiri, T. & Mizuno, M. Efficient method for the one-pot azidation of alcohols using bis(p-nitrophenyl) phosphorazidate. *Chem. Commun.* 2165–2166 (1997).

Acknowledgements

We thank the Swiss National Science Foundation for financial support (200021_182043 (K. G.) and 310030_197699 (P. S.)). Work in the laboratory of P. S. is supported by Swiss Lung Association (2018–02). We gratefully acknowledge the NMR- und MS-services of the University of Zurich and E. Jung (UZH) for discussions.

Author contributions

D. D., A. D., and K. G. designed the study. D. D. carried out the synthesis and characterization of the noviose modifications. A. D. carried out the synthesis and characterization of the rhamnose modifications. D. D., A. D., and K. G. analyzed data and discussed the results. D. S. and P. S. developed the MIC tests for *M. tuberculosis* and performed the biological evaluation of the derivatives against MTB. D. D., A. D., and K. G. wrote the manuscript.

Competing interests

The authors declare no competing interests.

Additional information

Supplementary information The online version contains supplementary material available at <https://doi.org/10.1038/s42004-021-00501-6>.

Correspondence and requests for materials should be addressed to K.G.

Reprints and permission information is available at <http://www.nature.com/reprints>

Publisher's note Springer Nature remains neutral with regard to jurisdictional claims in published maps and institutional affiliations.



Open Access This article is licensed under a Creative Commons Attribution 4.0 International License, which permits use, sharing, adaptation, distribution and reproduction in any medium or format, as long as you give appropriate credit to the original author(s) and the source, provide a link to the Creative Commons license, and indicate if changes were made. The images or other third party material in this article are included in the article's Creative Commons license, unless indicated otherwise in a credit line to the material. If material is not included in the article's Creative Commons license and your intended use is not permitted by statutory regulation or exceeds the permitted use, you will need to obtain permission directly from the copyright holder. To view a copy of this license, visit <http://creativecommons.org/licenses/by/4.0/>.

© The Author(s) 2021